

Production of ^{61}Ca , ^{63}Sc , ^{65}Ti , $^{68,69}\text{V}$, ^{71}Cr , ^{77}Fe , and ^{79}Co in projectile fragmentation with radioactive ion beams at 1A GeV

Na Tang,^{1,2} Bing Li,^{1,2} Jing-Jing Li,^{2,1} and Feng-Shou Zhang^{1,2,3,*}¹*The Key Laboratory of Beam Technology of Ministry of Education, College of Nuclear Science and Technology, Beijing Normal University, Beijing 100875, China*²*Institute of Radiation Technology, Beijing Academy of Science and Technology, Beijing 100875, China*³*Center of Theoretical Nuclear Physics, National Laboratory of Heavy Ion Accelerator of Lanzhou, Lanzhou 730000, China*

(Received 6 December 2022; accepted 19 December 2022; published 3 January 2023)

Projectile fragmentation provides an method to produce the unknown neutron-rich isotopes. In this work, the isospin-dependent Boltzmann-Langevin equation is employed to investigate the influence of projectiles on the fragments production. The cross sections of fragments with proton number $Z = 20\text{--}27$ are calculated under the reaction systems $^{81,84,86}\text{Ga} + ^9\text{Be}$. The obtained results suggest that the radioactive projectile ^{86}Ga is favorable to the yields of neutron-rich nuclei. The newly produced isotopes ^{61}Ca , ^{63}Sc , ^{65}Ti , $^{68,69}\text{V}$, ^{71}Cr , ^{77}Fe , and ^{79}Co , whose cross sections are characterized by the order of 1 to 100 μb , can be observed in the reaction $^{86}\text{Ga} + ^9\text{Be}$ at 1A GeV. This means the production cross sections of neutron-rich nuclei are very highly sensitive to the neutron-proton excess of projectile.

DOI: [10.1103/PhysRevC.107.014603](https://doi.org/10.1103/PhysRevC.107.014603)

I. INTRODUCTION

The landscape of the nuclide chart is a hot topic in nuclear physics, namely the investigation of the extensions to both the proton- and neutron-drip lines [1–7]. The new isotope ^{39}Na discovered at the RIKEN Nishina Center Radioactive Isotope Beam Factory has a significant impact on theories predicting the neutron drip line [8]. New half-lives of the neutron drip-line in the vicinity of $N \approx 28$ for $Z = 12\text{--}15$ were measured at the Facility for Rare Isotope Beams (FRIB) [9]. So far, the study of isotonic chains with $N = 50$ and their nearby nuclide has been located mainly in terra incognita, and even the existence of most nuclei has not yet been confirmed. The precise determination of nuclei far away from the β -stability line offers the access to explore the evolution of shell structure with extreme neutron-to-proton ratio [10,11].

As is well known, the nuclide with extreme neutron-to-proton excess is rarely observed in the terrestrial experiments. It attributes to that most of the fragmentation reactions are performed by using the stable projectile imping on a target [12,13]. For example, the reported neutron-rich isotopes $^{59,60}\text{Ca}$ and ^{62}Sc are produced from the fragmentation of a reaction system $^{70}\text{Zn} + ^9\text{Be}$ at 345A MeV in the radioactive ion-beam factory of the RIKEN Nishina Center [14–16]. Also, the eight new isotopes, namely ^{73}Mn , ^{76}Fe , $^{77,78}\text{Co}$, $^{80,81,82}\text{Ni}$, and ^{83}Cu , have been produced at the RIKEN Radioactive Isotope Beam Factory using a ^{238}U beam [17]. The study of projectile fragmentation in the $^{112}\text{Sn} + ^{112}\text{Sn}$, $^{124}\text{Sn} + ^{124}\text{Sn}$ [18], and $^{238}\text{U} + ^9\text{Be}$ reactions using the high-resolution performance of the projectile Fragment Separator at GSI [19]

were performed both at an incident energy of 1A GeV. Hence, it is more difficult to produce nuclei close to the drip line. This requires that the detected and separated capabilities of the experimental equipment should be further advanced.

With the development of the facilities, the radioactive ion beams (RIBs) of neutron-rich nuclei can be obtained [20–22]. The FRIB will offer unprecedented access to exotic nuclei. Experiments with the majority (80%) of the isotopes predicted to exist up to uranium ($Z = 92$) will become available [21,23–26]. Meanwhile, the FRIB linear accelerator is being prepared for upgrading to 400A MeV (FRIB400) [27]. The Système de Production d’Ions Radioactifs en Ligne-2 facility has been proposed at GANIL, the intensities should be expected to reach 10^9 pps for ^{132}Sn and ^{144}Xe and 10^{10} pps for ^{92}Kr in the future [28]. Facility for Antiprotons and Ion Research (FAIR) will be one of the biggest and most complex accelerator facilities worldwide. The particles will be accelerated up to about 90% of the speed of light in the FAIR accelerator facility and made use for scientific experiments [22]. The reported High Intensity heavy ion Accelerator Facility, which is a new generation accelerator in China, will provide stable and unstable heavy-ion beams with high intensity and energy [29,30]. The RIBs including ^{91}Kr (4×10^{11} pps), ^{142}Xe (9×10^9 pps), ^{132}Sn (7×10^{10} pps), and ^{81}Ga (1×10^9 pps) will be produced in the Beijing Isotope-Separation-On Line Neutron-Rich Beam Facility (BISOL), which can be used to explore the new physics at the limit of the nuclear stability in the intermediate mass region [31]. These RIBs provide an alternative access to the existence of more neutron-rich isotopes.

The production of unknown isotopes has been influenced by various reaction mechanisms, such as the projectile

*Corresponding author: fszhang@bnu.edu.cn

fragmentation [32–35], fission of actinide nuclide [36], fusion-evaporation reactions [37–39], and multinucleon transfer reactions [40–42], etc. As mentioned in Ref. [19], the projectile fragmentation method has been recognized as a dominant method in the production of the neutron-rich isotopes, especially the production for light [43,44] and heavy [45,46] neutron-rich nuclei at intermediate and high energies [47,48], respectively. Therefore, the fragmentation mechanism provides more distinct information to find the optimal combination in producing unknown nuclei.

Plenty of methods have been developed for calculating the fragmentation cross sections, such as the FRACS parametrization [49,50] and the empirical parametrization of fragmentation cross sections [51,52]. Currently, two kinds of transport codes have been used to simulate heavy-ion collisions reactions. One is the quantum molecular dynamics model [53–55] or the improved quantum molecular dynamics model [56–58]. Other is the Boltzmann-like model, which includes the Boltzmann-Uehling-Uhlenbeck (BUU) [59–61] and Boltzmann-Langevin equations (BLE) [62–66], etc. The nucleus-nucleus interactions are composed of the mean-field components and the two-body residual interactions in both of them. In contrast to the BUU model, the source of the fluctuations has been incorporated naturally into the BLE transport model. In order to further describe the isospin effects in the potential energy, the isospin-dependent Boltzmann-Langevin equation (IBLE) has been developed. The extended IBLE model offers a pronounced description of production cross sections in nuclear fragmentation reaction at intermediate and high energies [57,67–69].

The use of the RIBs is a most efficient approach to produce rare isotopes due to the large neutron excess of projectile [46]. The fragmentation reactions induced by neutron-rich nuclei can provide information about the isospin-dependent observables [70] and also make constrains on the equation of state of isospin asymmetric nuclear matter [71–73]. Particularly, accurate knowledge on nuclear cross sections for the production of $Z = 20\text{--}27$ radioisotopes is very important for the shell structure of the atomic nucleus; the production, propagation, and composition of cosmic rays; and technological applications [14,74]. In fact, the investigations of detailed information on these nuclide can give correct scaling of physical parameters, allowing a better understanding of the nucleus-nucleus collisions. Moreover, this provides a sensitive probe to comprehend the supernovas and neutron stars physics [75]. In this work, we aim at investigating the influence of neutron excess of projectile on the fragment production process based on the isospin-dependent Boltzmann-Langevin equation. Furthermore, the unknown neutron-rich isotopes with $Z = 20\text{--}27$ are investigated in the reaction $^{86}\text{Ga} + ^9\text{Be}$ at 1A GeV.

The article is organized as follows. In Sec. II, the isospin-dependent Boltzmann-Langevin model is briefly introduced. The results and discussion are presented in Sec. III. Finally, a conclusion is provided in Sec. IV.

II. THEORETICAL FRAMEWORK

The fragmentation reaction can be simulated successfully by the IBLE. In this model, the dynamical fluctuation has been

taken into account naturally due to the high-order correlations. The single-particle density $\hat{f}(\vec{r}, \vec{p}, t)$ is determined by the semiclassical one-body transport equation as follows [76,77]:

$$\left[\frac{\partial}{\partial t} + \frac{\vec{p}}{m} \cdot \nabla_{\vec{r}} - \nabla_{\vec{r}} U(\hat{f}) \cdot \nabla_{\vec{p}} \right] \hat{f}(\vec{r}, \vec{p}, t) = K(\hat{f}) + \delta K(\vec{r}, \vec{p}, t), \quad (1)$$

where the left-hand side describes the Vlasov propagation that is determined in terms of the nuclear mean field $U(\hat{f})$. The quantity $K(\hat{f})$ can be described by the fluctuating density $\hat{f}(\vec{r}, \vec{p}, t)$, which is the usual collision term with the Uehling-Uhlenbeck form,

$$K(\hat{f}) = \int d\vec{p}_2 d\vec{p}_3 d\vec{p}_4 W(12; 34) [\hat{f}_3 \hat{f}_4 (1 - \hat{f}_1)(1 - \hat{f}_2) - \hat{f}_1 \hat{f}_2 (1 - \hat{f}_3)(1 - \hat{f}_4)]. \quad (2)$$

Here $\hat{f}_i = \hat{f}(\vec{r}, \vec{p}_i, t)$ and $W(12; 34)$ is the transition rate. The quantity $\delta K(\vec{r}, \vec{p}, t)$ in Eq. (1) denotes the fluctuating collision term, which is similar to a random force term in a typical Langevin equation [76]. The amplitude of the fluctuations and the actual strength of friction are determined by a fluctuations-dissipation theorem [78,79]. Hence, the fluctuating collision term satisfies the correlation function, which can be written as:

$$\langle \delta K(\vec{r}_1, \vec{p}_1, t_1) \delta K(\vec{r}_2, \vec{p}_2, t_2) \rangle = C(\vec{p}_1, \vec{p}_2) \delta(\vec{r}_1 - \vec{r}_2) \delta(t_1 - t_2). \quad (3)$$

The angle brackets in above formula is a local average, which is performed over densities generated during a short time interval Δt [80,81]. The left side $\langle \delta K(\vec{r}_1, \vec{p}_1, t_1) \delta K(\vec{r}_2, \vec{p}_2, t_2) \rangle$ is assumed to be local in time and space, which is consistent with Markovian approximations in the Boltzmann collision term. $C(\vec{p}_1, \vec{p}_2)$ is the correlation function determined by the one-body properties of the locally averaged distribution $\hat{f}(\vec{r}, \vec{p}, t)$ and can be expressed in the weak-coupling limit [82].

In the IBLE model, the interaction potential of the system including isospin degree of freedom for nucleons can be written as

$$U_{\tau}(\rho, \delta, \vec{p}) = \alpha \frac{\rho}{\rho_0} + \beta \left(\frac{\rho}{\rho_0} \right)^{\gamma} + E_{\text{sym}}^{\text{loc}}(\rho) \delta^2 + \frac{\partial E_{\text{sym}}^{\text{loc}}(\rho)}{\partial \rho} \rho \delta^2 + E_{\text{sym}}^{\text{loc}}(\rho) \rho \frac{\partial \delta^2}{\partial \rho_{\tau}} + U_{\text{MDI}}, \quad (4)$$

where $\rho = \rho_n + \rho_p$ is the total nucleon density and $\delta = \frac{\rho_n - \rho_p}{\rho}$ denotes the isospin asymmetry. The quantities ρ_n and ρ_p are neutron and proton density, respectively. The exclusive parameters α and β distinguish the two- and three-body parts, γ is the compression coefficient determined by the nuclear matter. Two kinds of parameter sets are shown in Table I [54]. In this work, we apply the IBLE model with hard symmetry energy to calculate the production cross-sections of neutron-rich fragments in projectile fragmentation reactions.

TABLE I. Model parameters adopted in this work.

Parameters	α (MeV)	β (MeV)	γ	K (MeV)
Soft	-390	320	1.14	200
Hard	-130	59	2.09	380

The $E_{\text{sym}}^{\text{loc}}(\rho)$ is the local part of the symmetry energy, which can be expressed as [65]:

$$E_{\text{sym}}^{\text{loc}}(\rho) = \frac{1}{2} C_{\text{sym}} \left(\frac{\rho}{\rho_0} \right)^{\gamma_s}, \quad (5)$$

where $C_{\text{sym}} = 29.4$ MeV, $\gamma_s = 2.0$. The last term in the Eq. (4) is the momentum-dependent potential, which is given in Refs. [83,84],

$$U_{\text{MDI}} = \frac{t_4}{\rho_0} \int \hat{f}(\vec{r}, \vec{p}) \{ \ln[t_5(\vec{p} - \vec{p}')^2 + 1] \}^2 d\vec{p}'. \quad (6)$$

The parameters $t_4 = 15.7$ MeV, $t_5 = 0.0005$ MeV $^{-2}$. The nuclear symmetry energy (including the local part of symmetry energy and kinetic) in the subsaturated density region can be basically determined with different γ_s . We take $E_{\text{sym}}(\rho_0) = 30$ MeV in the present work.

The IBLE is a random equation of single particle density, which gives the ensemble of the single-particle density $\hat{f}(\vec{r}, \vec{p}, t)$. The purpose in solving IBLE is to investigate the phenomenon associated with the dynamical fluctuations in heavy-ion collisions at intermediate energy. Such as multifragmentation, which is related to the fluctuations of local densities. Therefore, we adopt an approximate method projecting fluctuations on the local multipole moments of the momentum distribution for simulating Eq. (1) [85,86]. We retain the multipole moments to the z component of the first two nonvanishing terms, quadrupole and octupole moment ($Q_{20} + Q_{30}$), which can be written as

$$\begin{aligned} Q_{20} &= \int dr d\mathbf{p} \hat{Q}_{20} \hat{f}(\mathbf{r}, \mathbf{p}, t) \\ &= \int dr d\mathbf{p} (2p_z^2 - p_x^2 - p_y^2) \hat{f}(\mathbf{r}, \mathbf{p}, t), \end{aligned} \quad (7)$$

$$\begin{aligned} Q_{30} &= \int dr d\mathbf{p} \hat{Q}_{30} \hat{f}(\mathbf{r}, \mathbf{p}, t) \\ &= \int dr d\mathbf{p} [p_z(2p_z^2 - 3p_x^2 - 3p_y^2)] \hat{f}(\mathbf{r}, \mathbf{p}, t). \end{aligned} \quad (8)$$

The coalescence model [87–90] can be used to construct clusters in the BLE simulation, which is a more convenient and much cheaper way. At the same time it also provides a full phase-space definition of fragments namely both in momentum and real spaces. The bound fragments to be found in coalescence, particle with relative momenta smaller than P_0 and relative distance smaller than R_0 are considered to belong to one cluster. The parameters P_0 and R_0 are adopted as 3.5 fm and 300 MeV/ c , respectively [76]. Calculations were performed with 20 test particles. For the produced light fragments, the difference between the cross sections before and after de-excitation is small, due to the excitation energy of fragments is not sufficient to evaporate neutrons. In this

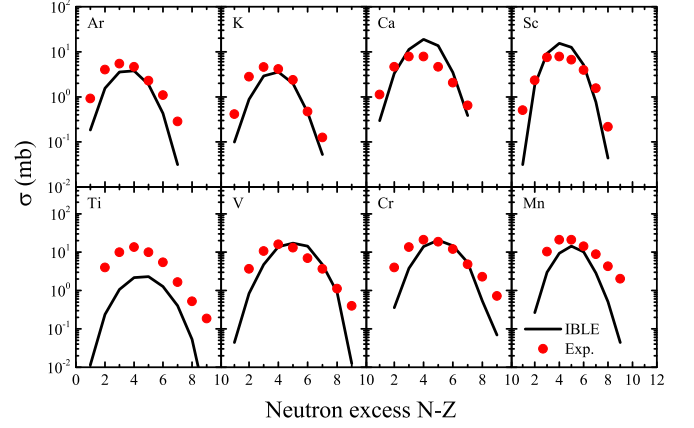


FIG. 1. Fragment cross sections plotted as a function of neutron excess in the reaction $^{69}\text{Cu} + ^9\text{Be}$ at 98.1 A MeV. The solid lines denote the calculated results obtained by the IBLE model, while the solid circle represents the experimental data coming from Ref. [46].

work, the production cross sections of light fragments around $Z = 20$ was mainly investigated.

III. RESULTS AND DISCUSSION

A. Comparison with experimental data

To facilitate the feasibility in predicting the production of neutron-rich nuclei, the fragment production cross sections of radioactive beam ^{69}Cu impinging on a target ^9Be at energy of about 98.1 A MeV have been reviewed. In Fig. 1, the cross sections of isotopes with proton number $Z = 18-25$ (black line) are plotted as a function of neutron excess. The solid circles represent the experimental data obtained from Ref. [46]. The systematical trend of theoretical results calculated by the IBLE model are almost consistent with the experimental data except the Ti isotopes that are underestimated by one order of magnitude. The peak values of isotope production cross sections increase with increasing charge number. A possible reason for this phenomenon is that fragments closed to the projectile are produced mainly by peripheral collisions. By contrast, central collision leads to the fragments further far away from the projectile. On the neutron-rich side, the results of our calculations are overall a better reproduction of the experimental database. In a word, the IBLE model provides a reliable approach to explore the projectile fragmentation reaction induced by radioactive beam. These results encourage us to forecast the unknown neutron-rich isotopes in the proceeding work.

B. Projectile dependence

In recent years, the development of the RIB technique has intrigued much more interest in both the experimental and theoretical nuclear reaction study induced by exotic nuclei. Therefore, the cross-section distributions of fragments produced under the reactions $^{81,84,86}\text{Ga} + ^9\text{Be}$ will be investigated at 1A GeV projectile energy. The half-lives of $^{81,84,86}\text{Ga}$ are 1221, 85, and 43 ms [91], respectively. The N/Z values for $^{81,84,86}\text{Ga}$ isotopes are 1.61, 1.71, and 1.77, respectively. The

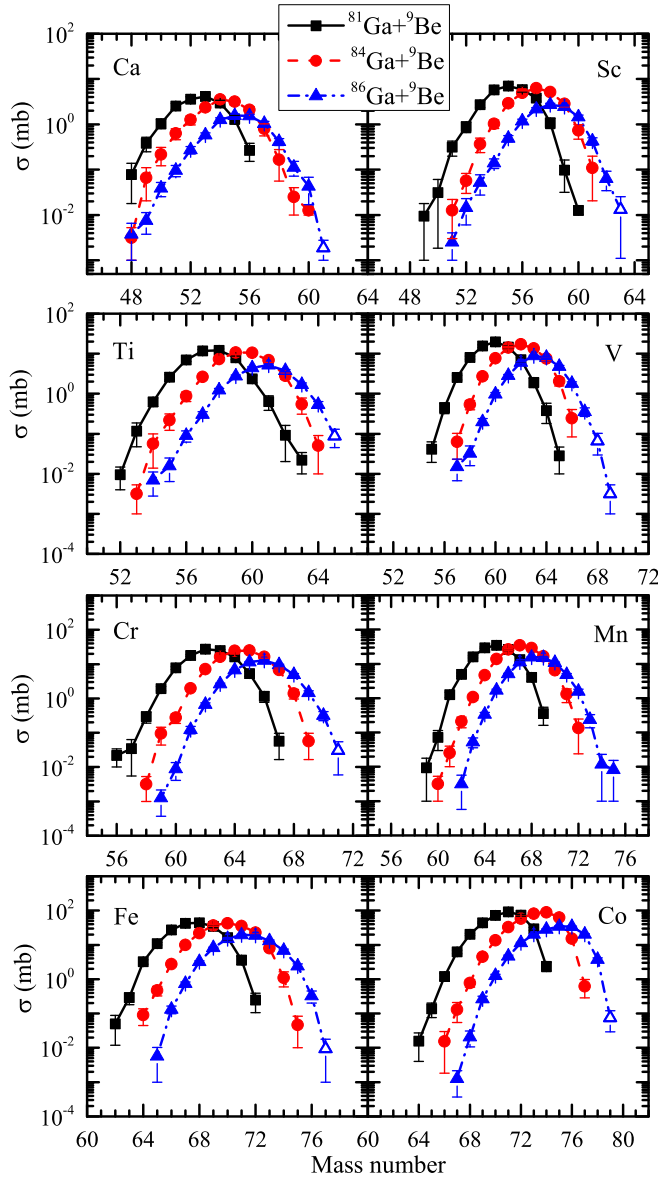


FIG. 2. The isotopic cross sections in the reactions $^{81,84,86}\text{Ga} + ^9\text{Be}$ at 1A GeV. The solid, dashed, and dash-dotted lines represent the result of these three reactions, respectively. Unknown nuclei are denoted by the open symbols.

asymmetric degree of freedom of projectile has an influence on the isotopic distributions in the fragmentation reaction [46,48]. Since it is essential to explore the isospin effect in these three reaction systems.

In Fig. 2, the cross sections of fragments with error bars produced in the $^{81,84,86}\text{Ga} + ^9\text{Be}$ reactions are plotted as a function of mass number. The solid, dashed, and dash-dotted lines represent the results obtained through these three reaction systems, respectively. Unknown nuclei are denoted by the open symbols. One can see that the isotopic distributions of fragment in these three reactions show similar shape expect the shift in mass number. This suggests that the isospin effect of projectile provides a sensitive probe to link the production cross section. The maximum value of the cross-section dis-

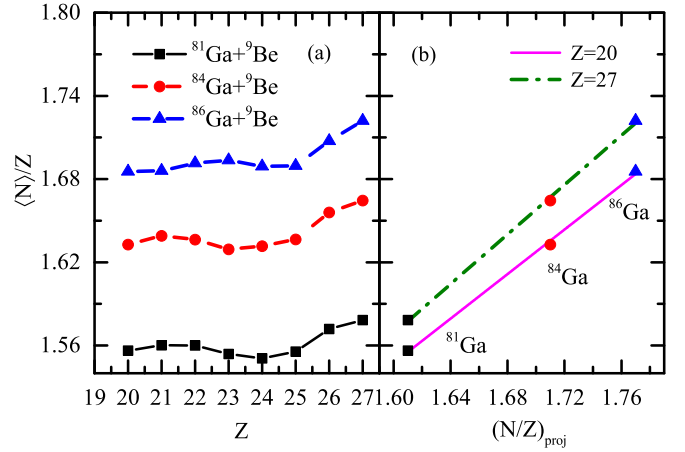


FIG. 3. (a) Mean $\langle N \rangle / Z$ ratio for reactions $^{81,84,86}\text{Ga} + ^9\text{Be}$. (b) The results for $Z = 20$ (solid line) and $Z = 27$ (dash-dotted line) as a function of the N/Z value of the projectile.

tributions becomes larger when the charge number of the fragment gradually close to the projectile. With increase of the neutron excess of the projectile, the location of peak value for isotopic production cross sections is decreased. However, it is obviously noted that the maximum of the isotopic distributions from ^{86}Ga -induced reaction has a shift toward the neutron rich side with respect to the $^{81,84}\text{Ga} + ^9\text{Be}$ reactions. By contrast, the shift becomes larger with the increasing neutron number in projectile. For instance, the centroids of the calcium isotope distributions for ^{81}Ga to ^{86}Ga projectiles shift by about two to three mass units. The widths of the isotopic distributions increase evidently with the added neutron number in the beams. In comparison with $^{81,84}\text{Ga} + ^9\text{Be}$, the $^{86}\text{Ga} + ^9\text{Be}$ system is more favorable to produce neutron-rich nuclei.

Remarkably note that the larger difference of the density distributions between neutrons and protons occurs in the surface region of the neutron-rich nucleus. The isospin effect in the projectile fragmentation are associated with the the density distributions of neutron and proton. The neutron-to-proton ratio of the final projectile-like fragmentation products is associated with the N/Z ratio of the projectile due to the excitation energy of the light primary fragments is not sufficient to wash off the neutron excess in the evaporation process. From isotope distributions, the mean neutron number for each Z can be obtained from $\langle N \rangle / Z = \sum_i N_i \sigma_i / \sum_i \sigma_i$, where N_i and σ_i are the neutron number and corresponding cross section, respectively [92]. The $\langle N \rangle / Z$ ratio for $^{81,84,86}\text{Ga}$ projectiles are shown in Fig. 3(a). A significant memory effect can be seen for the fragments close to the projectile, for they try to maintain the same isospin. The N/Z values of $^{81,84,86}\text{Ga}$ are much different and obvious difference has been observed for the $\langle N \rangle / Z$ ratio. Choosing particular elements, e.g., $Z = 20$ (solid line) and $Z = 27$ (dash-dotted line), are also enough to reveal the linear correlation of $\langle N \rangle / Z$ with the N/Z of the projectile [Fig. 3(b)]. Therefore, for a given projectile with larger neutron excess, the more neutron-rich nuclei can be produced in the fragmentation. Based on the relatively larger neutron excess, ^{86}Ga could be as a alternative radioactive

beam in producing neutron-rich nuclei for the forthcoming works.

By studying the projectile dependence, we also found that fragments close to the projectile, such as isotopes of iron and cobalt, exhibit an increasing peak in the isotopic reaction cross section. At the same time the cross sections of fragments located at the right of peak decrease with increasing neutron number. One of the reasons for this phenomenon is the effect of different impact parameters on the fragment isotopic cross sections. The cross sections of the fragments produced in the 1A GeV $^{86}\text{Ga} + ^9\text{Be}$ reaction within different impact parameters are calculated and the results are plotted in Fig. 4. The solid, dashed, and dash-dotted lines represent the result of the central collision ($0 < b < 3$), semiperipheral collision ($3 \leq b < 7$), and peripheral collision ($7 \leq b \leq b_{\text{max}}$), respectively. Roughly speaking, the fragments near the projectile are products of the semiperipheral and peripheral reactions, where the nucleus loses at most one proton and the excitation energy gained in the reaction leads to the evaporation of a few neutrons. On the other hand, the fragments further away from projectile are produced in the central collisions. For practical purposes, the neutron-rich projectiles and the peripheral reactions can be chosen in the planning of future experimental and theoretical studies.

C. Production of new isotopes ^{61}Ca , ^{63}Sc , ^{65}Ti , $^{68,69}\text{V}$, ^{71}Cr , ^{77}Fe , and ^{79}Co

The projectile has an influence on the production of isotopic cross sections. In order to reveal the new isotopes in the fragmentation reaction, the chosen system $^{86}\text{Ga} + ^9\text{Be}$ is investigated at the energy of 1A GeV. In order to further capture a glance of the nuclear chart, the nuclei region from $Z = 20$ to $Z = 27$ isotopes on the nuclear map is presented in Fig. 5. The filled and opened squares denoted the known and unknown nuclei, respectively. Blue square shows the β^- decay. The cross sections of the unknown of Ca, Sc, Ti, V, Cr, Fe, and Co isotopes in the reaction $^{86}\text{Ga} + ^9\text{Be}$ are shown in this figure. The anticipated 8 unknown isotopes can be find obviously from this nuclear map. The production cross sections for new nuclides ^{61}Ca is $1.88 \mu\text{b}$, ^{63}Sc is $13.2 \mu\text{b}$, ^{65}Ti is $87.3 \mu\text{b}$, $^{68,69}\text{V}$ are $65.9 \mu\text{b}$ and $3.14 \mu\text{b}$, ^{71}Cr is $30.14 \mu\text{b}$, ^{77}Fe is $9.42 \mu\text{b}$, and ^{79}Co is $74.7 \mu\text{b}$.

The κ ($\kappa = \sigma\phi$) is the main factor influences the event count rate in the detector, where the σ is the production cross section and ϕ is the beam intensity. The values of the factor κ of the isotopes Ca, Sc, Ti, V, Cr, Fe, and Co are plotted in Fig. 6. The unknown nuclei are marked as blank symbols. The ^{81}Ga beam intensity can reach 10^9 pps at the BISOL facility in the future [31]. The neutron-rich isotope ^{86}Ga was produced by projectile fission of ^{238}U at 750A MeV impinging on a ^9Be target [93]. The beam energy of the new third generation of radioactive nuclear beam facilities are up to 1A GeV. It makes it possible to use beams with large neutron-proton excess in experiments and improves the possibility of producing extremely rare isotopes. The discovery of ^{39}Na at RIKEN and the half-lives of exotic neutron-rich nuclei measured using the FRIB Decay Station initiator at FRIB demonstrate the advanced techniques and new science opportunities. They are

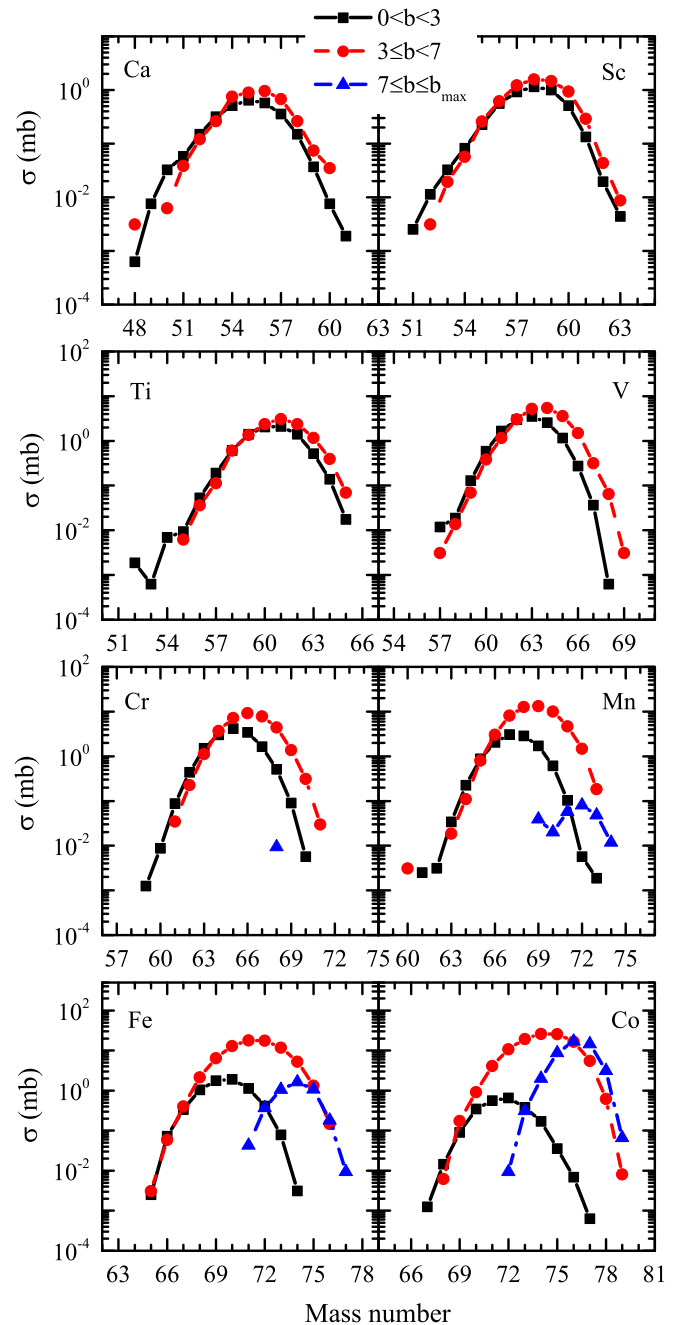


FIG. 4. Fragments produced in the 1A GeV $^{86}\text{Ga} + ^9\text{Be}$ reaction within different impact parameters b . The solid, dashed, and dash-dotted lines represent the result of the central, semiperipheral and peripheral collisions, respectively.

also most likely generated via projectile fragmentation in a newly built FRIB facility. The facility will achieve a dramatic increase in isotope production and allow the study of extreme neutron-rich nuclei. Hence, with the development of the new generation of RIB facilities, it is anticipated that the ^{86}Ga will reach the beam intensity of 10^9 pps in the future. The thickness of ^9Be target is usually 100 mg/cm^2 [94]. Based on the experimental conditions, the reaction $^{86}\text{Ga} + ^9\text{Be}$ at

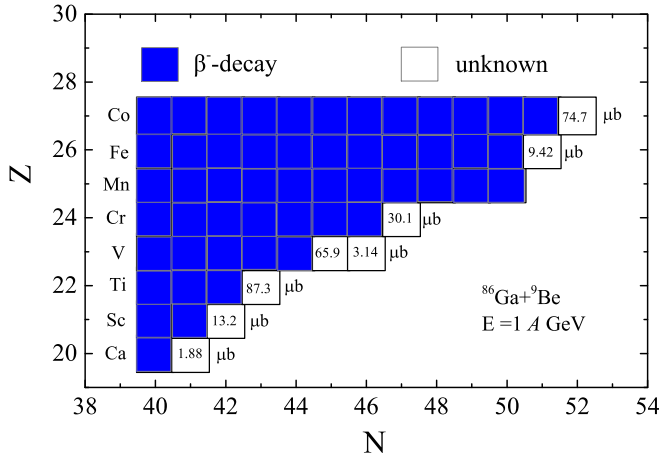


FIG. 5. The nuclei region from $Z = 20$ to $Z = 27$ on the nuclear map. The filled and open squares denote the known and unknown nuclei, respectively.

1A GeV is a potential candidate to produce unknown neutron-rich Ca, Sc, Ti, V, Cr, Fe, and Co isotopes.

IV. CONCLUSIONS

The IBLE can reproduce the cross sections of fragmentation in the $^{69}\text{Cu} + ^9\text{Be}$ reaction well. In comparison with the $^{81,84}\text{Ga} + ^9\text{Be}$ reactions, the larger production cross sections of neutron-rich nuclei can be obtained by the $^{86}\text{Ga} + ^9\text{Be}$ reaction due to the large neutron excess in the projectile. Therefore, ^{86}Ga can be regarded as an alternative radioactive beam to produce neutron-rich nuclei in the future. The cross sections of the Ca, Sc, Ti, V, Cr, Fe, Co, Ni, and Cu isotopes are explored in the reaction $^{86}\text{Ga} + ^9\text{Be}$. There are eight

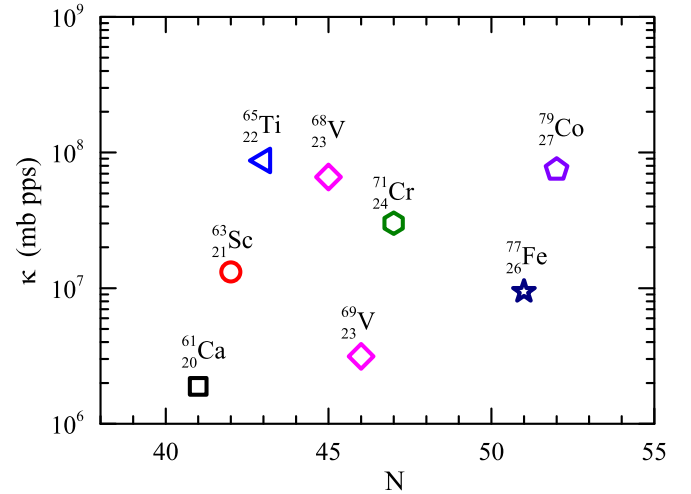


FIG. 6. Values of the factor $\kappa (= \sigma\phi)$ for the predicted Ca, Sc, Ti, V, Cr, Fe, and Co isotopes in the reaction $^{86}\text{Ga} + ^9\text{Be}$. σ is the production cross section, ϕ is the beam intensity. The blank symbols denote the predicted unknown nuclei.

unknown isotopes can be produced and the production cross sections of new isotopes ^{61}Ca is $1.88 \mu\text{b}$, ^{63}Sc is $13.2 \mu\text{b}$, ^{65}Ti is $87.3 \mu\text{b}$, $^{68,69}\text{V}$ are 65.9 and $3.14 \mu\text{b}$, ^{71}Cr is $30.14 \mu\text{b}$, ^{77}Fe is $9.42 \mu\text{b}$, and ^{79}Co is $74.7 \mu\text{b}$. Based on the experimental conditions, the reaction $^{86}\text{Ga} + ^9\text{Be}$ at 1A GeV provides a potential candidate to produce unknown neutron-rich isotopes of Ca, Sc, Ti, V, Cr, Fe, and Co.

ACKNOWLEDGMENTS

This work was supported by the National Natural Science Foundation of China under Grants No. 12135004, No. 11635003, and No. 11961141004.

- [1] <https://people.nsl.mscl.edu/~thoenness/isotopes> (2022).
- [2] M. Thoennessen, *The Discovery of Isotopes: A Complete Compilation* (Springer International Publishing, New York, 2016), pp. 1–384.
- [3] M. Thoennessen, *Int. J. Mod. Phys. E* **28**, 1930002 (2019).
- [4] M. Lewitowicz, R. Anne, G. Auger, D. Bazin, C. Borcea, V. Borrel, J. Corre, T. Dörfler, A. Fomichov, R. Grzywacz, D. Guillemaud-Mueller, R. Hue, M. Huyse, Z. Janas, H. Keller, S. Lukyanov, A. Mueller, Y. Penionzhkevich, M. Pfützner, F. Pougheon *et al.*, *Phys. Lett. B* **332**, 20 (1994).
- [5] C. Zeitlin, L. Heilbronn, J. Miller, S. E. Rademacher, T. Borak, T. R. Carter, K. A. Frankel, W. Schimmerling, and C. E. Stronach, *Phys. Rev. C* **56**, 388 (1997).
- [6] C. Sneden and J. J. Cowan, *Science* **299**, 70 (2003).
- [7] O. B. Tarasov, M. Portillo, A. M. Amthor, T. Baumann, D. Bazin, A. Gade, T. N. Ginter, M. Hausmann, N. Inabe, T. Kubo, D. J. Morrissey, A. Nettleton, J. Pereira, B. M. Sherrill, A. Stolz, and M. Thoennessen, *Phys. Rev. C* **80**, 034609 (2009).
- [8] D. S. Ahn, J. Amano, H. Baba, N. Fukuda, H. Geissel, N. Inabe, S. Ishikawa, N. Iwasa, T. Komatsubara, T. Kubo, K. Kusaka, D. J. Morrissey, T. Nakamura, M. Ohtake, H. Otsu,

- T. Sakakibara, H. Sato, B. M. Sherrill, Y. Shimizu, T. Sumikama *et al.*, *Phys. Rev. Lett.* **129**, 212502 (2022).
- [9] H. L. Crawford, V. Tripathi, J. M. Allmond, B. P. Crider, R. Grzywacz, S. N. Liddick, A. Andalib, E. Argo, C. Benetti, S. Bhattacharya, C. M. Campbell, M. P. Carpenter, J. Chan, A. Chester, J. Christie, B. R. Clark, I. Cox, A. A. Doetsch, J. Dopfer, J. G. Duarte *et al.*, *Phys. Rev. Lett.* **129**, 212501 (2022).
- [10] K. Langanke and M. Wiescher, *Rep. Prog. Phys.* **64**, 1657 (2001).
- [11] G. A. Souliotis, M. Veselsky, S. Galanopoulos, M. Jandel, Z. Kohley, L. W. May, D. V. Shetty, B. C. Stein, and S. J. Yennello, *Phys. Rev. C* **84**, 064607 (2011).
- [12] O. B. Tarasov, M. Portillo, D. J. Morrissey, A. M. Amthor, L. Bandura, T. Baumann, D. Bazin, J. S. Berryman, B. A. Brown, G. Chubarian, N. Fukuda, A. Gade, T. N. Ginter, M. Hausmann, N. Inabe, T. Kubo, J. Pereira, B. M. Sherrill, A. Stolz, C. Sumithrarachichi *et al.*, *Phys. Rev. C* **87**, 054612 (2013).
- [13] O. B. Tarasov, D. J. Morrissey, A. M. Amthor, T. Baumann, D. Bazin, A. Gade, T. N. Ginter, M. Hausmann, N. Inabe, T. Kubo, A. Nettleton, J. Pereira, M. Portillo, B. M. Sherrill, A. Stolz, and M. Thoennessen, *Phys. Rev. Lett.* **102**, 142501 (2009).

- [14] O. B. Tarasov, D. S. Ahn, D. Bazin, N. Fukuda, A. Gade, M. Hausmann, N. Inabe, S. Ishikawa, N. Iwasa, K. Kawata, T. Komatsubara, T. Kubo, K. Kusaka, D. J. Morrissey, M. Ohtake, H. Otsu, M. Portillo, T. Sakakibara, H. Sakurai, H. Sato *et al.*, *Phys. Rev. Lett.* **121**, 022501 (2018).
- [15] K. Helariutta, J. Benlliure, M. V. Ricciardi, and K. H. Schmidt, *Eur. Phys. J. A* **17**, 181 (2003).
- [16] J. Shergur, B. A. Brown, V. Fedoseyev, U. Köster, K. L. Kratz, D. Seweryniak, W. B. Walters, A. Wöhr, D. Fedorov, M. Hannawald, M. Hjorth-Jensen, V. Mishin, B. Pfeiffer, J. J. Ressler, H. O. U. Fynbo, P. Hoff, H. Mach, T. Nilsson, K. Wilhelmsen-Rolander, H. Simon *et al.*, *Phys. Rev. C* **65**, 034313 (2002).
- [17] T. Sumikama, S. Nishimura, H. Baba, F. Browne, P. Doornenbal, N. Fukuda, S. Franchoo, G. Gey, N. Inabe, T. Isobe, P. R. John, H. S. Jung, D. Kameda, T. Kubo, Z. Li, G. Lorusso, I. Matea, K. Matsui, P. Morfouace, D. Mengoni *et al.*, *Phys. Rev. C* **95**, 051601(R) (2017).
- [18] H. Imal, A. Ergun, N. Buyukcizmeci, R. Ogul, A. S. Botvina, and W. Trautmann, *Phys. Rev. C* **91**, 034605 (2015).
- [19] J. Kurcewicz, F. Farinon, H. Geissel, S. Pietri, C. Nociforo, A. Prochazka, H. Weick, J. Winfield, A. Estradé, P. Allegro, A. Bail, G. Bélier, J. Benlliure, G. Benzoni, M. Bunce, M. Bowry, R. Caballero-Folch, I. Dillmann, A. Evdokimov, J. Gerl *et al.*, *Phys. Lett. B* **717**, 371 (2012).
- [20] T. Kubo, M. Ishihara, N. Inabe, H. Kumagai, I. Tanihata, K. Yoshida, T. Nakamura, H. Okuno, S. Shimoura, and K. Asahi, *Nucl. Instrum. Methods B* **70**, 309 (1992).
- [21] <https://frib.msu.edu/> (2022).
- [22] <https://www.gsi.de/en/researchaccelerators/fair.htm> (2022).
- [23] T. Glasmacher, B. Sherrill, W. Nazarewicz, A. Gade, P. Mantica, J. Wei, G. Bollen, and B. Bull, *Nucl. Phys. News* **27**, 28 (2017).
- [24] M. Thoennessen, *Nucl. Data Sheets* **118**, 85 (2014).
- [25] G. Bollen, *AIP Conf. Proc.* **1224**, 432 (2010).
- [26] P. Ostroumov, M. Hausmann, K. Fukushima, T. Maruta, A. Plastun, M. Portillo, J. Wei, T. Zhang, and Q. Zhao, *J. Instrum.* **15**, P12034 (2020).
- [27] P. Ostroumov, C. Contreras, A. Plastun, J. Rathke, T. Schultheiss, A. Taylor, J. Wei, M. Xu, T. Xu, Q. Zhao, I. Gonin, T. Khabiboulline, Y. Pischalnikov, and V. Yakovlev, *Nucl. Instrum. Methods Phys. Res., Sect. A* **888**, 53 (2018).
- [28] S. Gales, *Prog. Part. Nucl. Phys.* **59**, 22 (2007).
- [29] J. Yang, J. Xia, G. Xiao, H. Xu, H. Zhao, X. Zhou, X. Ma, Y. He, L. Ma, D. Gao, J. Meng, Z. Xu, R. Mao, W. Zhang, Y. Wang, L. Sun, Y. Yuan, P. Yuan, W. Zhan, J. Shi *et al.*, *Nucl. Instrum. Methods B* **317**, 263 (2013).
- [30] P. Liu, J. H. Chen, Y. G. Ma, and Z. Song, *Nucl. Sci. Tech.* **28**, 55 (2017).
- [31] Y. L. Ye, *EPJ Web Conf.* **178**, 01005 (2018).
- [32] H. Sakurai, N. Aoi, A. Goto, M. Hirai, N. Inabe, M. Ishihara, H. Kobinata, T. Kubo, H. Kumagai, T. Nakagawa, T. Nakamura, M. Notani, Y. Watanabe, Y. Watanabe, and A. Yoshida, *Phys. Rev. C* **54**, R2802 (1996).
- [33] M. Fauerbach, D. J. Morrissey, W. Benenson, B. A. Brown, M. Hellström, J. H. Kelley, R. A. Kryger, R. Pfaff, C. F. Powell, and B. M. Sherrill, *Phys. Rev. C* **53**, 647 (1996).
- [34] O. B. Tarasov, T. Baumann, A. M. Amthor, D. Bazin, C. M. Folden III, A. Gade, T. N. Ginter, M. Hausmann, M. Matos, D. J. Morrissey, A. Nettleton, M. Portillo, A. Schiller, B. M. Sherrill, A. Stolz, and M. Thoennessen, *Phys. Rev. C* **75**, 064613 (2007).
- [35] M. Veselsky, *Phys. Rev. C* **74**, 054611 (2006).
- [36] T. Ohnishi, T. Kubo, K. Kusaka, A. Yoshida, K. Yoshida, M. Ohtake, N. Fukuda, H. Takeda, D. Kameda, K. Tanaka, N. Inabe, Y. Yanagisawa, Y. Gono, H. Watanabe, H. Otsu, H. Baba, T. Ichihara, Y. Yamaguchi, M. Takechi, S. Nishimura *et al.*, *J. Phys. Soc. Jpn.* **79**, 073201 (2010).
- [37] L. Zhu, Z. Q. Feng, C. Li, and F. S. Zhang, *Phys. Rev. C* **90**, 014612 (2014).
- [38] J. J. Li, C. Li, G. Zhang, L. Zhu, Z. Liu, and F. S. Zhang, *Phys. Rev. C* **95**, 054612 (2017).
- [39] A. K. Nasirov, G. Mandaglio, G. Giardina, A. Sobiczewski, and A. I. Muminov, *Phys. Rev. C* **84**, 044612 (2011).
- [40] C. Li, F. Zhang, J. J. Li, L. Zhu, J. Tian, N. Wang, and F. S. Zhang, *Phys. Rev. C* **93**, 014618 (2016).
- [41] L. Zhu, F. S. Zhang, P. W. Wen, J. Su, and W. J. Xie, *Phys. Rev. C* **96**, 024606 (2017).
- [42] X. R. Zhang, G. Zhang, J. J. Li, S. H. Cheng, Z. Liu, and F. S. Zhang, *Phys. Rev. C* **103**, 024608 (2021).
- [43] B. A. Bian, F. S. Zhang, and H. Y. Zhou, *Nucl. Phys. A* **807**, 71 (2008).
- [44] D. Pérez-Loureiro, J. Benlliure, H. Álvarez Pol, B. Blank, E. Casarejos, D. Dragosavac, V. Föhr, M. Gascón, W. Gawlikowicz, A. Heinz, K. Helariutta, A. Kelić-Heil, S. Lukić, F. Montes, L. Pieńkowski, K. H. Schmidt, M. Staniou, K. Subotić, K. Sümmerer, J. Taieb *et al.*, *Phys. Lett. B* **703**, 552 (2011).
- [45] H. Alvarez-Pol, J. Benlliure, E. Casarejos, L. Audouin, D. Cortina-Gil, T. Enqvist, B. Fernández-Domínguez, A. R. Junghans, B. Jurado, P. Napolitani, J. Pereira, F. Rejmund, K. H. Schmidt, and O. Yordanov, *Phys. Rev. C* **82**, 041602(R) (2010).
- [46] S. Lukyanov, M. Mocko, L. Andronenko, M. Andronenko, D. Bazin, M. A. Famiano, A. Gade, S. P. Lobastov, W. G. Lynch, A. M. Rogers, O. B. Tarasov, M. B. Tsang, G. Verde, M. S. Wallace, and R. G. T. Zegers, *Phys. Rev. C* **80**, 014609 (2009).
- [47] M. Veselsky, R. W. Ibbotson, R. Laforest, E. Ramakrishnan, D. J. Rowland, A. Ruangma, E. M. Winchester, E. Martin, and S. J. Yennello, *Phys. Rev. C* **62**, 064613 (2000).
- [48] R. Ogul, A. S. Botvina, U. Atav, N. Buyukcizmeci, I. N. Mishustin, P. Adrich, T. Aumann, C. O. Bacri, T. Barczyk, R. Bassini, S. Bianchin, C. Boiano, A. Boudard, J. Brzyczyk, A. Chbihi, J. Cibor, B. Czech, M. De Napoli, J.-E. Ducret, H. Emling *et al.*, *Phys. Rev. C* **83**, 024608 (2011).
- [49] B. Mei, *Phys. Rev. C* **95**, 034608 (2017).
- [50] Y. D. Song, H. L. Wei, C. W. Ma, and J. H. Chen, *Nucl. Sci. Tech.* **29**, 96 (2018).
- [51] K. Sümmerer, *Phys. Rev. C* **86**, 014601 (2012).
- [52] K. Sümmerer and B. Blank, *Phys. Rev. C* **61**, 034607 (2000).
- [53] E. Lehmann, R. K. Puri, A. Faessler, G. Batko, and S. W. Huang, *Phys. Rev. C* **51**, 2113 (1995).
- [54] J. Aichelin, *Phys. Rep.* **202**, 233 (1991).
- [55] C. Hartnack, R. K. Puri, J. Aichelin, J. Konopka, S. A. Bass, H. Stöcker, and W. Greiner, *Eur. Phys. J. A* **1**, 151 (1998).
- [56] J. Su, L. Zhu, and E. Xiao, *Phys. Rev. C* **105**, 024608 (2022).
- [57] H. Wolter, M. Colonna, D. Cozma *et al.*, *Prog. Part. Nucl. Phys.* **125**, 103962 (2022).
- [58] J. Su, F. S. Zhang, and B. A. Bian, *Phys. Rev. C* **83**, 014608 (2011).
- [59] B. Blättel, V. Koch, W. Cassing, and U. Mosel, *Phys. Rev. C* **38**, 1767 (1988).

- [60] J. Aichelin, *Phys. Rev. C* **33**, 537 (1986).
- [61] G. Verde, P. Danielewicz, D. A. Brown, W. G. Lynch, C. K. Gelbke, and M. B. Tsang, *Phys. Rev. C* **67**, 034606 (2003).
- [62] S. Ayik and C. Gregoire, *Phys. Lett. B* **212**, 269 (1988).
- [63] F. S. Zhang and E. Suraud, *Phys. Lett. B* **319**, 35 (1993).
- [64] B. A. Bian, F. S. Zhang, and H. Y. Zhou, *Chin. Phys. Lett.* **24**, 1529 (2007).
- [65] W. J. Xie, J. Su, L. Zhu, and F. S. Zhang, *Phys. Lett. B* **718**, 1510 (2013).
- [66] W. J. Xie, J. Su, L. Zhu, and F. S. Zhang, *Phys. Rev. C* **88**, 061601(R) (2013).
- [67] S. Ayik and C. Grégoire, *Nucl. Phys. A* **513**, 187 (1990).
- [68] J. Randrup and B. Remaud, *Nucl. Phys. A* **514**, 339 (1990).
- [69] B. Li, N. Tang, Y. H. Zhang, and F. S. Zhang, *Nucl. Sci. Tech.* **33**, 55 (2022).
- [70] R. Ogul and A. S. Botvina, *Phys. Rev. C* **66**, 051601(R) (2002).
- [71] B. A. Li, L. W. Chen, and C. M. Ko, *Phys. Rep.* **464**, 113 (2008).
- [72] D. V. Shetty, S. J. Yennello, and G. A. Souliotis, *Phys. Rev. C* **76**, 024606 (2007).
- [73] P. Napolitani, M. Colonna, F. Gulminelli, E. Galichet, S. Piantelli, G. Verde, and E. Vient, *Phys. Rev. C* **81**, 044619 (2010).
- [74] G. Hagen, M. Hjorth-Jensen, G. R. Jansen, R. Machleidt, and T. Papenbrock, *Phys. Rev. Lett.* **109**, 032502 (2012).
- [75] A. R. Raduta and F. Gulminelli, *Phys. Rev. C* **82**, 065801 (2010).
- [76] F. S. Zhang and E. Suraud, *Phys. Rev. C* **51**, 3201 (1995).
- [77] B. Li, N. Tang, and F. S. Zhang, *Chin. Phys. C* **45**, 084103 (2021).
- [78] G. van der Zwan and P. Mazur, *Physica A* **98**, 169 (1979).
- [79] R. Kubo, *Rep. Prog. Phys.* **29**, 255 (1966).
- [80] P. G. Reinhard and E. Suraud, *Ann. Phys.* **216**, 98 (1992).
- [81] P. G. Reinhard, E. Suraud, and S. Ayik, *Ann. Phys.* **213**, 204 (1992).
- [82] E. Suraud, S. Ayik, M. Belkacem, and J. Stryjewski, *Nucl. Phys. A* **542**, 141 (1992).
- [83] J. Aichelin, A. Rosenhauer, G. Peilert, H. Stoecker, and W. Greiner, *Phys. Rev. Lett.* **58**, 1926 (1987).
- [84] Z. Q. Feng, *Nucl. Phys. A* **878**, 3 (2012).
- [85] Y. Abe, S. Ayik, P. G. Reinhard, and E. Suraud, *Phys. Rep.* **275**, 49 (1996).
- [86] E. Suraud, S. Ayik, M. Belkacem, and F. S. Zhang, *Nucl. Phys. A* **580**, 323 (1994).
- [87] H. Kruse, B. V. Jacak, J. J. Molitoris, G. D. Westfall, and H. Stöcker, *Phys. Rev. C* **31**, 1770 (1985).
- [88] C. W. Chen, F. S. Zhang, and G. M. Jin, *Phys. Rev. C* **58**, 2283 (1998).
- [89] L. W. Chen, F. S. Zhang, G. M. Jin, and Z. Y. Zhu, *Phys. Lett. B* **459**, 21 (1999).
- [90] F. S. Zhang, L. W. Chen, Z. Y. Ming, and Z. Y. Zhu, *Phys. Rev. C* **60**, 064604 (1999).
- [91] G. Rudstam and E. Lund, *Phys. Rev. C* **13**, 321 (1976).
- [92] X. H. Zhang, Z. Y. Sun, R. F. Chen, Z. Q. Chen, Z. Y. Guo, J. L. Han, Z. G. Hu, T. H. Huang, R. S. Mao, Z. G. Xu, M. Wang, J. S. Wang, Y. Wang, G. Q. Xiao, H. S. Xu, X. H. Yuan, H. B. Zhang, X. Y. Zhang, and T. C. Zhao, *Phys. Rev. C* **85**, 024621 (2012).
- [93] M. Bernas, C. Engelmann, P. Armbruster *et al.*, *Phys. Lett. B* **415**, 111 (1997).
- [94] M. Mocko, M. B. Tsang, L. Andronenko, M. Andronenko, F. Delaunay, M. Famiano, T. Ginter, V. Henzl, D. Henzlová, H. Hua, S. Lukyanov, W. G. Lynch, A. M. Rogers, M. Steiner, A. Stolz, O. Tarasov, M. J. van Goethem, G. Verde, W. S. Wallace, and A. Zalessov, *Phys. Rev. C* **74**, 054612 (2006).